J. Astrophys. Astr. (1997) **18,** 407–414

An Analysis of 900 Rotation Curves of Southern Sky Spiral Galaxies: Do Rotation Curves Fall into Discrete Classes?

D. F. Roscoe, *School of Mathematics, Sheffield University, Sheffield, S3 7RH, UK*
Email: D.Roscoe@ac.shef.uk

Abstract. One of the largest rotation curve data bases of spiral galaxies currently available is that provided by Persic & Salucci (1995; hereafter, PS) which has been derived by them from unreduced rotation curve data of 965 southern sky spirals obtained by Mathewson, Ford & Buchhorn (1992; hereafter, MFB). Of the original sample of 965 galaxies, the observations on 900 were considered by PS to be good enough for rotation curve studies, and the present analysis concerns itself with these 900 rotation curves.

The analysis is performed within the context of the hypothesis that velocity fields within spiral discs can be described by generalized power-laws. Rotation curve data was found to impose an extremely strong and detailed correlation between the free parameters of the power-law model, and this correlation accounts for virtually all the variation in the pivotal diagram. In the process, the analysis reveals completely unexpected structure which indicates that rotation curves can be partitioned into well-defined discrete subclasses.

Key words. Spiral galaxies—rotation curves.

1. Introduction

The following analysis is performed within the context of a prediction arising from a theory of weak-field slow-motion gravitation in material distributions that motions in spiral discs conform to the power-law structure

$$V_{\rm rot} = AR^{\alpha}, \quad V_{\rm rad} = BR^{\alpha}, \quad \alpha \geq -1, \tag{1}$$

where $V_{\rm rot}$ and $V_{\rm rad}$ are the rotational velocity and radial velocity respectively, and for constants A and B; since one of these can be absorbed into the scaling of the problem, it can be assumed that there are only two free parameters, (A, α) say. A crucial result, from the point of view of reconciling this result with the observations, is the constraint $\alpha \geq -1$, a result which immediately removes any mystery associated with the existence of 'flat' rotation curves.

The foregoing solution was derived purely from an analysis of the dynamics, with mass-conservation being ignored. However, the additional constraint of mass-conservation can do no more than impose an additional constraint on the space of solutions (1). This amounts to a correlation being imposed on the free-parameters, (A, α), of the model, and it can be shown that the existence of a perfect correlation

would imply the model is exact for the physics. However, rotation-curve data was extremely noisy, and so we cannot expect perfect correlations; it follows that, since perfect correlations cannot be expected, the whole argument revolves around the *quality* of any correlations uncovered.

2. The data

The data given by PS was obtained from the raw $H\alpha$ data of MFB by deprojection, folding and cosmological redshift correction. For any given galaxy, the data was presented in the form of estimated rotational velocities plotted against angular displacement from the galaxy's centre; estimated linear scales are not given and no data-smoothing is performed.

The analysis proposed here requires the linear scales of the galaxies in the sample to be defined which, in turn, requires distance estimates of the sample galaxies from our own locality. This information is given in the original MFB paper in the form of a Tulley-Fisher (TF hereafter) distance estimate given in km/sec, and assumes H = 85 km/sec/Mpc for the conversion. We have assumed:

- that the MFB method of presenting TF distances in km/sec, including their use of H = 85 km/sec/Mpc, gives an accurate estimate to the cosmological component of the redshift in the sample galaxies. This assumption is actually central to MFB's analysis since this analysis was primarily designed to give accurate determinations of peculiar velocities in the sample;
- that the criteria by which RFT selected, observed and processed their very much smaller sample ensured relatively accurate determinations of the corresponding cosmological redshifts.

Given these assumptions, then nominal agreement between the RFT and MFB linear scales can be obtained by converting the MFB distances, as quoted in km/sec, to a linear scale using the RFT value of H = 50km/sec/Mpc.

An analysis of the distribution of morphological types in the PS data base shows that the great majority of the selected galaxies are of types 3,4,5 and 6, with only two examples of types 0,1,2 and a tail of 31 examples of types 7,8,9. To maximise the homogeneity of the analysed data, the distribution tails – consisting of the morphological types 0,1,2,7,8 & 9 – were omitted, and the remaining 867 galaxies partitioned into the classes {3}, {4,5} and {6}. These contained, respectively, 306, 177 and 384 galaxies. A separate analysis was performed on each of these three partitions.

3. Is there any correlation between A and α?

The basic assumption is simply that rotation velocities behave as $V_{\text{rot}} = AR^{\alpha}$ and the discussion of § 1 concluded there should be a correlation between A and α. Since the regression constants arising from a linear regression of $\ln(V_{\text{rot}})$ on $\ln(R)$ give estimates of In (A) and α, our basic analysis performs a linear regression on each of the 867 rotation curves, and records the pair (α, $\ln(A)$) for each galaxy.

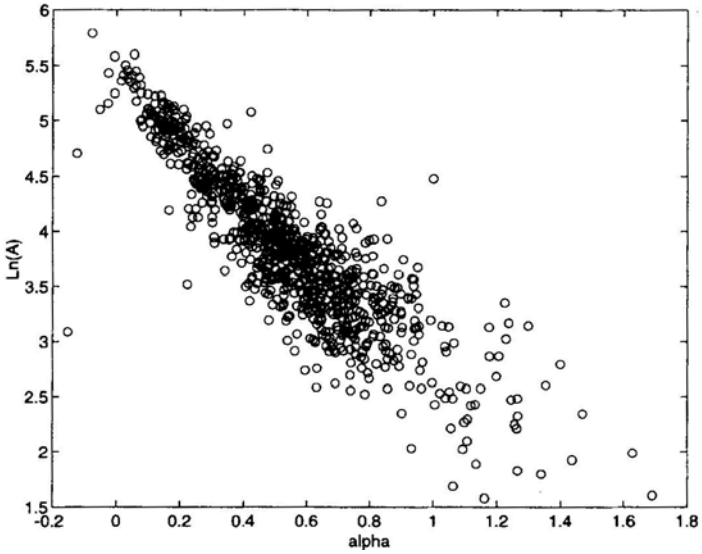

Figure 1. Plot of ln(A) against α for whole sample.

Fig. 1 gives the scatter plot of (α, ln(A)) for the full sample and shows that there exists an extremely strong negative (α, ln(A)) correlation. The corresponding figures for the individual galaxy typeclasses (not shown) are similar in all respects, each occupying similar areas in their respective (α, ln(A)) planes and each displaying the same fanlike structure going from a broad spread of points at the bottom right-hand of the figure to a narrow neck at the top left-hand of the figure. For the remainder of this paper, discussion will be restricted to the type-class {6} (that is, late-types) galaxies, since the conclusions arising here are broadly repeated in the two remaining classes.

4. A simple linear hypothesis

An obvious hypothesis to construct on Fig. 1 is that

$$\ln(A) = a_0 + b_0\alpha, \tag{2}$$

where a_0 and b_0 are constants which might differ between different type-classes. It is easily shown how this implies that the rotation curves underlying Fig. 1, $\ln(V_{\rm rot}) = \ln(A) + \alpha \ln(R)$, say, intersect at the fixed point $(-b_0, a_0)$ in the (ln(R),ln(V)) plane. Consequently, if (2) is a realistic model, all of the Fig. 1 rotation curves will *transform into each other* under rotations about $(-b_0, a_0)$ in this plane; that is, the individual rotation curves underlying Fig. 1 are equivalent to within a rotation about $(-b_0, a_0)$ in the (ln(R), ln(V)) plane. This geometric interpretation provides a means of testing the simple linear hypothesis, (2): Suppose linear regression on Fig. 1 yields the regression constants (a_0, b_0) for (2); then, if the assumption of linearity is reasonable, an arbitrarily chosen straight line passing through $(-b_0, a_0)$ in the (ln(R), ln(V)) plane can be defined as a standard 'reference line' into which each rotation curve underlying Fig. 1 can be transformed by a simple bulk-rotation about $(-b_0, a_0)$. Since, according to this idea, the rotation curves are reduced to equivalence by the

rotation, then the process of forming an 'average rotation curve' from the set of rotated such curves should greatly reduce the internal noise associated with the individual rotation curves, and we would expect the resulting average curve to be a very close fit to the standard reference line, referred to above.

In practice, this process was applied separately to the three typeclasses defined in §2 and the simple linear hypothesis (2) was strongly supported for the class-type {6} only; it was unsupported for the remaining two classes. It was concluded that hypothesis (2) gives a partially successful resolution of the data, but is inadequate for the task of giving a comprehensive resolution of the data.

5. The linear-fan model

Whilst the results of § 4 show (2) to be inadequate, they do suggest it might be considered a first-order approximation to some higher-order reality. With this in mind, recall the point made in § 3 that, apart from demonstrating a strong inverse correlation between α and $\ln(A)$, Fig. 1 also manifests a strong fan-like structure – going from a broad distribution of points at the bottom right-hand of the figure to a narrow neck of points at the top left-hand of the figure – which is reproduced in the corresponding figures for each of the individual galaxy typeclasses. The overall structure of this distribution is consistent in a qualitative, but obvious, way with the idea of the single linear relationship (2) for each galaxy type-class being replaced by a *discrete set* of linear relationships

$$\ln(A) = a_i + b_i\alpha, \quad i = 1, 2, \ldots \tag{3}$$

for each type-class, where the parameters (a_i, b_i) of the individual lines are such that these lines can be considered to converge somewhere in the region of (0.1,5.0) in the $(\alpha, \ln(A))$ plane of the class. This image, of a *linear fan* converging on a single point (or at least, in a small region), has the advantage of being strongly testable.

To arrive at this test, simply note that, when a set of straight lines, $y = mx + c$ in the (x, y) plane, are constrained so that all pass through a *fixed* point, (x_0, y_0) say, then the parameters (m, c) of the lines are constrained to satisfy $c = y_0 - x_0m$. In the present case, the refined hypothesis is that a set of linear relationships like (3) underlies each of the classes combined in Fig. 1, and that the lines in each of these sets are constrained to meet at a single point in the $(\alpha, \ln(A))$ plane; consequently, if this hypothetical point is denoted as $(\alpha_0, \ln(A_0))$ then, according to the hypothesis, the sets of parameters (a_i, b_i), $i = 1, 2, \ldots$ in (3) must be constrained to lie on the line

$$a = \ln(A_0) - \alpha_0 b. \tag{4}$$

So, the proposed test of the hypothesis is to show that there exists a set of parameters (a_i, b_i), $i = 1, 2, \ldots$, each one defining a fixed point in the $(\ln(R), \ln(V))$ plane, which are constrained by a relation of this type where, as Fig. 1 indicates, $(\alpha_0, \ln(A_0)) \approx (0.1, 5.0)$ for each of the type-classes {6}, {4,5} & {3}.

6. Testing the linear-fan model

In order to test the linear-fan model hypothesis, it is firstly necessary to determine the locations of individual points in the hypothesised class. The method hinges on the

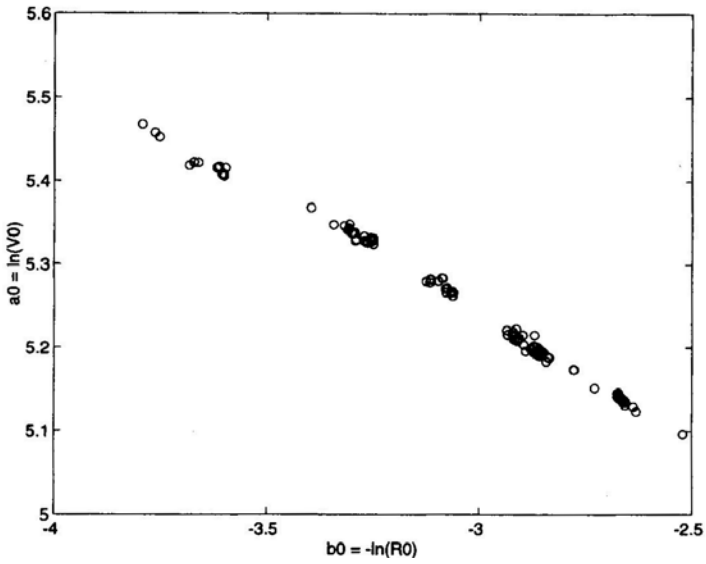

Figure 2. Fixed points in the linear fan model for type 6 spirals.

fact that the problem of locating the single fixed point, $(-b_0, a_0)$, could have been defined as a minimisation problem in which the sum of least-square residuals arising from rotating all the rotation curves about $(-b_0, a_0)$ so that they coincided with a reference line in a least-square sense, was minimised wrt the position of $(-b_0, a_0)$. Now, if the original hypothesis, (2), did, in fact, reflect accurately the actual situation, then it is to be expected that using the minimization procedure to locate the fixed point $(-b_0, a_0)$ should make little difference (within statistical noise) to its position calculated by regressing $\ln(A)$ on α (the procedure used in § 3); this is simply because the original hypothesis, of a single fixed point, amounts to the assumption that this fixed-point is a *global minimum* in the system and so there could only be one solution to the minimization process. However, if the linear-fan model provides a better description of the actual situation, then it is to be expected that using a minimization procedure with global searching should lead to the location of a class of distinct fixed-points.

The results of this search for galaxy type-class {6}, and for local minima $(-b_i, a_i)$, i =0, 1, 2,… satisfying $(-4 \le b_i \le -0.5)$ are shown in Fig. 2; the undisplayed results are similar in all respects. The figure consists of several tightly clumped masses of the symbol o', each denoting a successfully located minimum point. We interpret each such clumped mass to represent a *single* local minimum, with the scatter within each such clump arising from the noisy nature of the data. The figure provides conclusive evidence for a relationship like (4) being imposed on a *discrete* class of fixed points, $(-b_i, a_i)$, i = 0, 1, 2, … in the $(\ln(R), \ln(V))$ plane; consequently, that part of the refined hypothesis which asserts that the component classes combined in Fig. 1 can be understood in terms of the class of linear relationships

$$\ln(A) = a_i + b_i\alpha, i = 1, 2, \ldots \tag{5}$$

where the parameters (a_i, b_i), i = 1, 2, … are constrained by

$$a = \ln(A_0) - \alpha_0 b, \tag{6}$$

where $(\alpha_0, \ln(A_0))$ is fixed for each of the galaxy typeclasses, is confirmed for the subset of minima satisfying $(-4.0 \leq b_i \leq -2.5)$. However, there is also a quantitative aspect to the refined hypothesis which asserts that $(\alpha_0, \ln(A_0)) \approx (0.1,5.0)$ for each type-class. An estimate for the position of $(\alpha_0, \ln(A_0))$ for type-class {6} is found from a linear regression on the distribution of Fig. 2, and this gives, for the explicit representations of (6),

$$\text{Type 6:} \quad a = 4.347 - 0.298b. \tag{7}$$

so that $(\alpha_0, \ln(A_0))$ is given by (0.298, 4.347). The remaining two classes give (0.222, 4.625) and (0.162, 4.898) respectively. Each of these is close to the hypothesised approximate position (0.1, 5.0), and so the refined hypothesis can be considered confirmed in both its qualitative and quantitative aspects.

7. Interpretation and implication of results

It was shown in § 4 how the hypothesis (2), that the structures underlying Fig. 1 could each be understood in terms of a single linear relationship like (2), implied that, for each type-class under consideration, the rotation curves passed through a single fixed point in the $(\ln(R), \ln(V))$ plane, and were therefore equivalent to within a rotation about that point. However, (2) was rejected and replaced by the refinement of the linear-fan model which asserts the existence of a *discrete* class of such fixed points per galaxy class, and this refinement has been confirmed in § 6. This implies that, within each galaxy type-class, there are distinct subclasses of galaxies; each of these subclasses is defined by a fixed point in the $(\ln(R), \ln(V))$ plane (that is, the distinct points in Fig. 2) through which all the rotation curves of the galaxies in the subclass pass, and about which the rotation curves are equivalent to within a rotation.

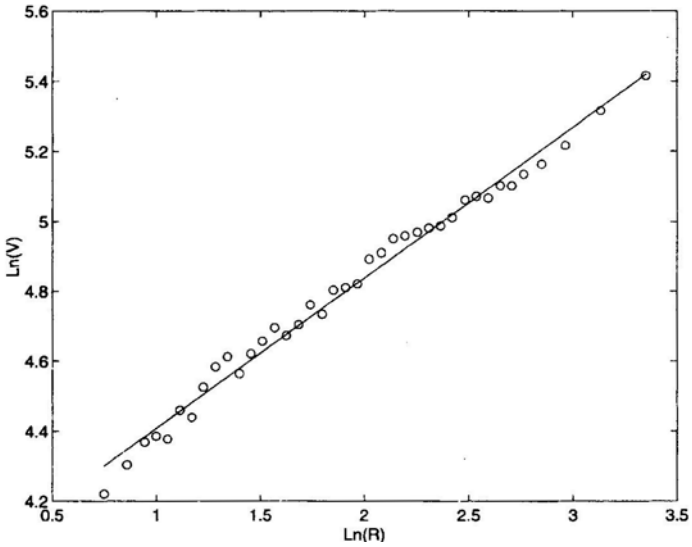

Figure 3. Averaged raw rotation-curve data for type 6 spirals.

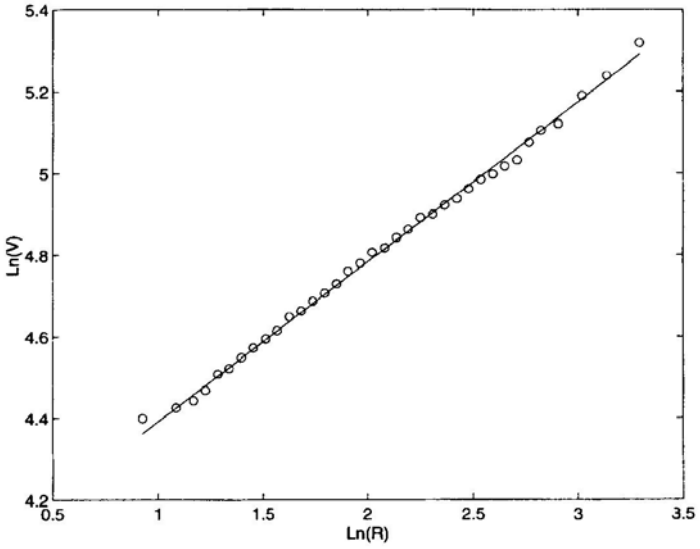

Figure 4. Averaged rotated rotation-curve data for type 6 spirals.

In principle, the galaxies could be sorted into these distinct subclasses and the rotation-averaging process described in § 4 performed on the rotation curves within each subclass; however, for the purposes of illustration, that fixed point giving the deepest minimum in the whole set of fixed points for the galaxy type-class has been selected as representative, and the rotation-averaging process on the *whole* type-class has been performed about this single fixed point. For type-class {6} the chosen fixed-point in the (ln(*R*), ln(*V*)) plane is (3.615, 5.416), and the corresponding rotated and averaged data over all the rotation-curves in the type-class is shown in Fig. 4. The scatter present in Fig. 3, which presents the averaged *unrotated* data over all type-class {6} rotation curves, is virtually eliminated. The results for the remaining sub-classes are strongly similar. This provides the strongest possible evidence for the idea of the equivalence of rotation curves with respect to rotations about particular fixed points in the (ln(*R*),ln(*V*)) plane.

To summarize, the 'linear-fan' model, that the components of Fig. 1 are each best understood in terms of a *discrete* class of converging linear relationships, (5) with (6), has been verified in quantitative detail; since this model manifestly accounts for virtually all of the variation in Fig. 1 then rotation curve data also provides the strong evidence supporting the general power-law model (1).

8. Conclusions

The presented analysis is based on the hypothesis that velocity fields in spiral discs can be described by a generalized power-law, and we argued that the extent to which rotation-curve data imposes correlations on the free parameters of the model provides a measure of quality for this hypothesis.

The considerations of § 3 to § 7 place the existence of a very strong and detailed correlation between the model parameters beyond all doubt; this correlation, which

has been termed herein as the 'linear-fan' model, accounts for virtually all the variation in Fig. 1 and so it can be concluded that rotation-curve data provides very strong evidence supporting the basic power-law model for spiral discs.

The details of this analysis lead to the conclusion (Fig. 2 and un-shown figures) that, within any given galaxy type-class, the galaxies fall into discrete subclasses, where each such subclass is defined by its association with a unique fixed point in the $(\ln(R), \ln(V))$ plane through which the rotation curves of the galaxies in the subclass *all* pass. This implies that all of the rotation curves concerned are equivalent to within a rotation about the fixed point, and this property is given a dramatic confirmation in the comparison of Fig. 3 with Fig. 4.

In conclusion, the discrete nature of the structures revealed by the data when analysed within the context of the generalized power-law has such profound implications for our understanding of gravity on the large scale that, ideally, this analysis should be repeated for Northern sky spirals.

References

Mathewson, D. S., Ford, V. L., Buchhorn, M. 1992, *Astrophys J. Suppl.,* **81**, 413.
Persic, M., Salucci, P. 1995, *Astrophys. J. Suppl.,* **99**, 501.